

Monitoring the vascular response and resistance to sunitinib in renal cell carcinoma *in vivo* with susceptibility contrast MRI

Running Title: Imaging RCC vascular response and resistance to sunitinib

Simon P. Robinson¹, Jessica K.R. Boulton¹,
Naveen S. Vasudev^{2†}, Andrew R. Reynolds^{2¶}

¹Cancer Research UK Cancer Imaging Centre, Division of Radiotherapy & Imaging, The Institute of Cancer Research, London, UK

²Tumour Biology Team, The Breast Cancer Now Toby Robins Research Centre, The Institute of Cancer Research, London, UK

Correspondence to: Simon P. Robinson
Division of Radiotherapy & Imaging
The Institute of Cancer Research,
London, SM2 5NG, UK.

Tel: 0208 722 4528
Fax: 0208 661 0846
e-mail: Simon.Robinson@icr.ac.uk

[†]Present address: Leeds Institute of Cancer and Pathology,
St James's University Hospital,
Leeds, LS9 7TF, UK

[¶]Present address: Early Clinical Development,
Innovative Medicines and Early Development,
AstraZeneca,
Cambridge, UK

Keywords: renal cell carcinoma, angiogenesis, sunitinib, resistance, MRI,

The authors declare no potential conflicts of interest

We acknowledge the support of Cancer Research UK (C1090/A16464) to the Cancer Imaging Centre at ICR, in association with the MRC and Department of Health (England), Breast Cancer Now, and the RMH/ICR/Mount Vernon Cancer Centre Academic Partnership Challenge Fund.

Abstract

Anti-angiogenic therapy is efficacious in metastatic renal cell carcinoma (mRCC). However, the ability of anti-angiogenic drugs to delay tumor progression and extend survival is limited, due to either innate or acquired drug resistance. Furthermore, there are currently no validated biomarkers that predict which mRCC patients will benefit from anti-angiogenic therapy. Here we exploit susceptibility contrast magnetic resonance imaging (SC-MRI) using intravascular ultrasmall superparamagnetic iron oxide particles to quantify and evaluate tumor fractional blood volume (fBV) as a non-invasive imaging biomarker of response to the anti-angiogenic drug sunitinib. We also interrogate the vascular phenotype of RCC xenografts exhibiting acquired resistance to sunitinib. SC-MRI of 786-0 xenografts prior to and two weeks after daily treatment with 40mg/kg sunitinib revealed a 71% ($p<0.01$) reduction in fBV in the absence of any change in tumor volume. This response was associated with significantly lower microvessel density ($p<0.01$) and lower uptake of the perfusion marker Hoechst 33342 ($p<0.05$). The average pre-treatment tumor fBV was negatively correlated ($R^2=0.92$, $p<0.0001$) with sunitinib-induced changes in tumor fBV across the cohort. SC-MRI also revealed suppressed fBV in tumors that acquired resistance to sunitinib. In conclusion, SC-MRI enabled monitoring of the anti-angiogenic response of 786-0 RCC xenografts to sunitinib, which revealed that pre-treatment tumor fBV was found to be a predictive biomarker of subsequent reduction in tumor blood volume in response to sunitinib, and acquired resistance to sunitinib was not associated with a parallel increase in tumor blood volume.

Introduction

Anti-angiogenic therapy has shown considerable efficacy in metastatic renal cell carcinoma (mRCC) (1). Newly diagnosed mRCC patients are now treated with vascular endothelial growth factor (VEGF) receptor tyrosine kinase inhibitors (sunitinib or pazopanib) as standard of care (2, 3). Approximately 80% of patients with mRCC achieve an initial period of disease control with these agents, whilst ~20% of patients derive no benefit. However, even responding patients inevitably progress due to acquired resistance that typically develops after a period of several months on treatment (4). Two modes of resistance to anti-angiogenic therapy are thus currently recognised; innate resistance, whereby the tumor fails to respond to the therapy from the outset, and acquired resistance, whereby after a period of response to therapy the tumor begins to regrow (5, 6). Both forms of resistance may arise due to the presence of alternative mechanisms of tumor vascularisation, which are VEGF-independent, and allow the tumor to evade the effects of the targeted agent. These mechanisms are however poorly understood, and there are currently no validated biomarkers that predict which mRCC patients will benefit from anti-angiogenic therapy.

Non-invasive imaging approaches that facilitate the detection of changes in tumor biology may form the basis for improved predictive biomarkers. Advances in imaging technologies provide a means of defining quantitative biomarkers to inform on biologically relevant structure-function relationships in tumors (7). Such imaging methods enable a better understanding of the behaviour and heterogeneous distribution of such associations, and inform on response and resistance to treatment (8). In addition to quantifying any therapy-induced volumetric change *in vivo*, functional imaging methods can also provide additional mechanistic insight.

Perfusion computed tomography (CT), and dynamic contrast-enhanced (DCE) magnetic resonance imaging (MRI) using low molecular weight gadolinium chelates, have been widely

used to assess patients with mRCC and response to VEGF signalling inhibitors (9). However, these clinical studies suffered from marked measurement variability, particularly with DCE MRI. Alternative functional MRI techniques are thus being evaluated to provide more specific imaging biomarkers for the assessment of tumor vascular function and response *in vivo*. One approach, susceptibility contrast MRI, involves measuring the uptake and distribution of intravenously administered ultrasmall superparamagnetic iron oxide (USPIO) particles, composed primarily of an iron (Fe^{3+}) oxide crystalline core with a biocompatible coating (10). USPIO particles create large susceptibility effects that increase the transverse MRI relaxation rate R_2^* , and whose long intravascular half-life enables steady-state, high-resolution measurements of R_2^* (11). Quantitation of fractional blood volume (fBV, %), derived from measurements of the absolute increase in tumor R_2^* following the administration of USPIO particles, provides a sensitive imaging biomarker of response to vascular targeted therapies (12-14).

The mechanisms of resistance to anti-angiogenic therapy can be investigated using preclinical cancer models. We have previously established that subcutaneous xenografts of the 786-0 renal cancer cell line can demonstrate resistance to sunitinib treatment (15). The aims of this study were to (i) evaluate fBV derived from susceptibility contrast MRI as a non-invasive predictive imaging biomarker of 786-0 xenograft response *in vivo*, and (ii) interrogate the vascular phenotype of 786-0 xenografts exhibiting acquired resistance to sunitinib.

Materials & Methods

Cell culture, tumor propagation, drug formulation and treatment

Human 786-0 RCC cells (ATCC, LCG Standards; purchased 2011) were cultured in RPMI 1640 medium supplemented with 10% foetal bovine serum (Invitrogen, Paisley, UK) and maintained at 37°C in a humidified incubator with an atmosphere of 95% air, 5% CO₂. Resuscitated cells were cultured for ~2-3 weeks prior to injection into mice. Cells tested negative for mycoplasma infection and cell line authenticity was confirmed by short tandem repeat (STR) typing (15).

All *in vivo* experiments were performed in accordance with the local ethical review panel, the UK Home Office Animals (Scientific Procedures) Act 1986, the United Kingdom National Cancer Research Institute guidelines for the welfare of animals in cancer research (16), and the ARRIVE guidelines (17). Adult female CB17/SCID mice (*CB17/lcr-Prkdc^{scid}/lcrIcoCrI*, Charles River, UK) were injected subcutaneously in the right flank with 3x10⁶ 786-0 cells. Animals were housed in specific pathogen-free rooms in autoclaved, aseptic microisolator cages with a maximum of four animals per cage. Food and water were provided *ad libitum*. The mice were routinely monitored for the appearance of palpable tumors. Established tumors were enrolled into the study when volumes reached ~250mm³, as assessed by callipers, using the formula for an ellipsoid volume, $(L \times W^2)/2$, where L and W were the two largest dimensions of the ellipsoid.

Sunitinib was formulated in 0.5% carboxymethyl cellulose, 300mM NaCl, 0.4% Tween-80 and 0.9% benzyl alcohol adjusted to pH 6.0, as previously described (18).

Mice bearing established 786-0 xenografts underwent MRI prior to and following two weeks of daily oral treatment with 40mg/kg sunitinib. Following the post-treatment scan, tumors were excised, fixed in formalin (10% (v/v) neutral buffered formalin) and embedded in paraffin for subsequent immunohistochemistry. Additional untreated tumors were used to

provide control/reference tissue for histological analysis.

An additional six tumor-bearing mice that were not imaged prior to treatment but exhibited acquired resistance to daily treatment with sunitinib, designated 786-0-R, were imaged by MRI when their tumors reached at least 4x their volume at commencement of treatment.

MRI data acquisition and analysis

MRI was performed on a 7T horizontal bore microimaging system (Bruker, Ettlingen, Germany) using a 3cm birdcage volume coil. Anaesthesia was induced with a 10ml/kg intraperitoneal injection of fentanyl citrate (0.315mg/ml) plus fluanisone (10mg/ml (Hypnorm; Janssen Pharmaceutical Ltd., High Wycombe, UK)), midazolam (5mg/ml (Hypnovel; Roche)), and sterile water (used at a ratio of 1:1:2). A lateral tail vein was cannulated with a 27G butterfly catheter (Hospira, Royal Leamington Spa, Warwickshire, UK) for remote administration of USPIO particles. Mice were positioned in the coil on a custom-built platform to isolate the tumor, and their core temperature was maintained at 37°C with warm air blown through the magnet bore.

Contiguous multi-slice T₂-weighted 1mm thick axial images were first acquired for tumor localisation and volume determination. Multiple gradient-recalled echo (MGRE) T₂*-weighted images were then acquired from three 1mm thick axial slices across each tumor using a 128x128 matrix over a 3cmx3cm field of view (FOV), with repetition time (TR)=200ms, 8 echo times (TE) of 6 to 27ms spaced 3.14ms apart, and 8 averages, giving an overall acquisition time of ~3½ minutes. A dose of 150µmolFe/kg of the USPIO particle preparation P904[®] (overall particle size ~25-30nm diameter, Guerbet, Villepinte, France) was then administered intravenously and, after 3 minutes to allow for equilibration, a second set of identical MGRE images acquired.

Image analysis was performed using in-house software (Imageview, developed in IDL, ITT

Visual Information Systems, Boulder, CO, USA). Tumor volumes were determined using segmentation from regions of interest (ROI's) drawn on T₂-weighted images for each tumor-containing slice. Tumor R₂^{*} maps were calculated from the MGRE images acquired prior to and following administration of USPIO particles by fitting a single exponential to the signal intensity echo time curve on a voxel-by-voxel basis using a Bayesian maximum *a posteriori* approach (19). Parametric maps of tumor fBV (%) were subsequently calculated using the USPIO-induced change in R₂^{*} (ΔR_2^*), as previously described (14, 20).

Immunohistochemistry and fluorescence microscopy

Immunohistochemical detection of endomucin was used to assess tumor microvessel density (MVD) (15). Formalin-fixed paraffin-embedded (FFPE) sections were incubated with rat monoclonal anti-endomucin antibodies (#SC65495, Santa Cruz, Heidelberg, Germany), and immunoreactivity detected with biotinylated anti-rat IgG secondary antibodies and a DAB substrate kit (Vector, Burlingame, CA, USA). Slides were counterstained with haematoxylin prior to mounting in DEPEX, and visualised on a BX51 microscope (Olympus Optical, London, UK). Endomucin positive vessels were counted in 5 randomly selected high-power fields (x100) for each tumor and the number converted into vessels/mm².

Separate cohorts of mice bearing 786-0 xenografts treated for 2 weeks with 40mg/kg/day sunitinib or vehicle control were injected via a lateral tail with the perfusion marker Hoechst 33342 (Sigma-Aldrich, Poole, UK) (21). After 1 minute, tumors were rapidly excised and snap frozen over liquid nitrogen. Fluorescence signals from Hoechst 33342 were subsequently detected above a constant threshold at 365nm from 10 μ m thick frozen whole tumor sections (3 per tumor) using a motorised scanning stage (Prior Scientific Instruments, Cambridge, UK) attached to the BX51 microscope, driven by image analysis software (CellP, Soft Imaging System, Münster, Germany). The area of each tumor section with Hoechst 33342 fluorescence was determined and expressed as a percentage of the whole tumor area, as previously described (12, 22).

Statistics

All statistical analyses were performed using GraphPad Prism version 6.07. Results are presented in the form mean \pm 1 s.e.m. Following application of a Shapiro-Wilk normality test to confirm the Gaussian distribution of the data, significance testing employed Student's two-tailed t-test, assuming unequal variances with a 5% level of significance. Significant correlations were determined using linear regression analysis.

Results

Susceptibility contrast MRI with USPIO particles measures fractional tumor blood volume of 786-0 xenografts

Susceptibility contrast MRI incorporating the use of USPIO particles was used to assess the perfused vasculature of subcutaneous 786-0 xenografts. The schematic data in Supplementary Figure 1 shows a T₂-weighted anatomical image (Supplementary Fig 1a), gradient-recalled echo (GRE) images prior to and post administration of USPIO particles (Supplementary Fig 1b,c) and the calculated parametric fractional blood volume (fBV) map (Supplementary Fig 1d) obtained from a representative 786-0 xenograft. These data show that successful injection and delivery of USPIO particles into the tumor intravascular compartment resulted in a clear reduction in GRE image intensity in perfused tumor areas allowing calculation of a parametric fBV map. Furthermore, administration of USPIO particles resulted in no noticeable adverse effects to the mice or tumor growth, and no significant difference in tumor baseline R₂* measured prior to and post-treatment, indicating no sequestration of USPIO particles that could influence subsequent fBV measurements.

Tumor fBV maps obtained from a representative mouse bearing a 786-0 xenograft prior to and 2 weeks after daily treatment with 40mg/kg sunitinib are shown in Figure 1a and 1b. A marked reduction in fBV was consistently observed post-treatment, which was primarily associated with the tumor core. The fBV cumulative frequency curves for the same 786-0 xenograft pre- and post-treatment revealed a marked left shift in distribution towards smaller values, with a substantial increase in the proportion of voxels with fBV below 5% following treatment (Figure 1c). Susceptibility contrast MRI revealed a reduction in fBV in 8 of 9 treated tumors (Figure 1d), resulting in a significant (p<0.01) 70% reduction in the cohort mean fBV in the absence of any significant change in cohort mean tumor volume (Table 1). This response was associated with a significant (p<0.01) reduction in microvessel density (MVD), as assessed by immunohistochemical detection of endomucin positive vessels (Figure 2a), and significantly (p<0.05) reduced perfusion as evidenced by lower Hoechst

33342 uptake (Figure 2b), in the sunitinib-treated cohort relative to control. Positive endomucin staining and Hoechst 33342 fluorescence was seen predominantly at the periphery of tumors in the sunitinib-treated mice.

Pre-treatment fractional tumor blood volume is predictive of the anti-angiogenic response to sunitinib in 786-0 xenografts

The data in Figure 1d suggests that tumors exhibiting a relatively high pre-treatment fBV subsequently showed the greatest reduction in fBV after 2 weeks daily treatment with sunitinib. By simply plotting the average baseline fBV against the treatment-induced change in fBV after 2 weeks, a correlation would be expected even when there may be no relationship (23). To overcome this, and test whether the baseline fBV was indeed predictive for the subsequent reduction in fBV in response to sunitinib, the average of the final and mean baseline fBV was plotted against the change in fBV (Δ fBV) measured after 2 weeks treatment for each tumor (Figure 3a). A highly significant and strong negative correlation was obtained ($R^2=0.92$, $p<0.0001$), greater than the correlation of 0.7 that would be expected by chance (23). There was no significant relationship between sunitinib-induced reduction in fBV with change in tumor volume (Figure 3b), pre-treatment tumor fBV with pre-treatment tumor volume or sunitinib-induced reduction in fBV with pre-treatment tumor volume (data not shown).

Acquired resistance to sunitinib is not associated with a parallel increase in tumor fractional blood volume in 786-0 xenografts

Notably, in six tumor-bearing mice, we observed a period of growth control during the early phase of sunitinib treatment, which was followed by tumor re-growth whilst still on treatment (Supplementary Fig 2a). This is similar to the phenomenon of acquired drug resistance that can be seen in mRCC patients treated with sunitinib in the clinic. Susceptibility contrast MRI data was also acquired from these 786-0-R xenografts that exhibited acquired resistance to

sunitinib. Here, acquired resistance was defined as a four-fold increase in tumor volume compared to the tumor volume at the day treatment started, and which was observed at a median of 75 days post initiation of daily treatment (range = 62 to 99 days). Representative parametric fBV maps acquired from two 786-0-R xenografts are shown in Figure 4a. Note the far larger cross-sectional area/appearance of the progressing tumors on MRI compared to that in Figure 1. The quantitative volumetric and fBV data obtained from the 786-0-R cohort are summarised in Figure 4b and c, and Table 1, with that obtained from the 786-0 cohort pre- and post-treatment shown for comparison. Collectively these data clearly show that, surprisingly, the progressing 786-0-R xenografts maintained a suppressed fBV.

Discussion

The initial response and subsequent relapse of mRCC patients treated with VEGF receptor tyrosine kinase inhibitors such as sunitinib is well documented (4). Currently there are no validated biomarkers that accurately predict which mRCC patients will benefit from anti-angiogenic therapy, and the mechanisms associated with the innate and acquired resistance are poorly understood. In this pre-clinical study, quantitation of tumor fractional blood volume (fBV) using susceptibility contrast MRI was evaluated (i) for its potential as a non-invasive predictive imaging biomarker of 786-0 xenograft response to sunitinib, and (ii) to quantify the degree of functional vascularisation of 786-0 xenografts exhibiting acquired resistance to chronic treatment with sunitinib, *in vivo* (15).

Susceptibility contrast MRI yielded a pre-treatment mean fBV of ~8% in untreated 786-0 xenografts, consistent with similar measurements reported across a range of subcutaneous rodent tumor models using different USPIO preparations (12, 14, 24, 25). Daily treatment with sunitinib for 2 weeks induced a marked reduction in the fBV of 786-0 xenografts *in vivo*, with tumor uptake of USPIO particles, and therefore patent vasculature, restricted to the tumor periphery post-treatment. Importantly, this response was associated with histologically confirmed reduction in MVD and perfused vessels, providing strong validation of fBV as a quantitative imaging biomarker of functional tumor vasculature, and its response to sunitinib, in this model of RCC (7). Similar reductions in tumor fBV, measured by susceptibility contrast MRI, have been reported following treatment with other anti-vascular therapies (12, 14, 24, 26-28). The data provides further support for the clinical development and application of USPIO particles for the assessment of human tumor vasculature and its response to treatment. Recent studies have highlighted the efficacy and safety of the USPIO particle preparation ferumoxytol for MRI investigations in both adults and children (29-31), and in imaging-embedded oncology clinical trials (32).

RCC 786-0 xenografts exhibiting a relatively larger fBV subsequently showed the greatest

reduction in fBV in response to sunitinib. Furthermore, a strong and highly significant negative correlation between baseline tumor fBV and its subsequent response to daily treatment with sunitinib over 2 weeks was obtained, suggesting that baseline fBV has prognostic value for subsequent tumor vascular response to sunitinib, and is a predictor of the magnitude of the reduction in fBV following treatment. The absence of any correlation of sunitinib-induced change in fBV with changes in tumor volume re-iterates the shortcomings of the RECIST criteria to correctly assess human tumor response to anti-angiogenic therapies, and the need for robust non-invasive vascular imaging readouts (33).

In the clinic, perfusion CT and DCE MRI, and the quantitative biomarkers they provide (Hounsfield unit (HU) of density and the volume transfer constant K^{trans} , respectively), have been predominantly used to assess patients with mRCC and response to VEGF signalling inhibitors (9). Several imaging-embedded investigations reported that highly vascular renal tumors had a beneficial outcome following treatment (34-37), and that early reductions in HU and K^{trans} related to subsequent beneficial survival (34, 38, 39). Marked measurement variability, particularly in K^{trans} , was apparent in these clinical studies, likely a consequence of different pharmacokinetic modelling approaches used to analyse the CT and DCE MRI data. The data herein strongly suggest that quantitation of fBV using susceptibility contrast MRI may provide a simpler, more sensitive and specific imaging biomarker for predicting and assessing the vascular response of mRCC in the clinic. In this regard, the potential of arterial spin-labelling MRI, which is wholly non-invasive and yields absolute quantitation of tissue blood flow (mls/100g/min), has also been highlighted (40, 41).

Until recently, remarkably few pre-clinical studies have exploited relapsing and/or acquired resistant tumor models to study mechanisms of resistance to targeted therapies. One reason for this is the inherent longevity, and hence practical implications, associated with developing a resistant phenotype in xenografts *in vivo*. However, the radiology and quantitative imaging biomarkers in such models are likely to provide more accurate pre-

clinical platforms for evaluating both novel therapeutics and drug resistance. We recently described the development of a 786-0 RCC xenograft model of acquired resistance to daily dosing with sunitinib, with tumors exhibiting late resistance ~2-3 months after treatment initiation (15). In the present study, susceptibility contrast MRI clearly revealed impaired fBV in progressing 786-0-R xenografts *in vivo* (see also Supplementary Figure 2).

A rebound in tumor angiogenesis, mediated by VEGF-independent mechanisms, has been suggested as one mechanism by which tumors may evade anti-angiogenic therapy (5, 6). However, this has been predicated on numerous studies that have relied on histopathological determination of tumor vessel density, and have not incorporated any direct measure of perfused/functional tumor vasculature *in vivo*. Our non-invasive susceptibility contrast MRI data obtained in 786-0 xenografts demonstrate that acquired resistance to sunitinib is not associated with functional re-vascularisation *in situ*, and suggest that tumors can gain acquired resistance to anti-angiogenic therapy without the need to induce rebound angiogenesis.

How do we explain why acquired resistance to anti-angiogenic therapy can be observed without an accompanying rebound re-vascularisation? Tumor adaptation to treatment with VEGF signalling inhibitors may involve a metabolic adaptation in cancer cells, which permits cancer cells to survive despite a treatment-induced reduction in tumor vasculature and the associated hypoxic environment (42, 43). Intriguingly, we recently demonstrated that sunitinib-resistant 786-0 tumor xenografts are more hypoxic than parental 786-0 xenografts *in vivo* (44). Furthermore, metabolic symbiosis between tumor cells distal and proximal to surviving vessels has also been recently implicated in acquired resistance to sunitinib in RCC (45). Therefore, it appears possible that the 786-0-R xenografts analysed in the current study can acquire resistance to anti-angiogenic therapy, without recourse to rebound re-vascularisation, because there is a shift in tumor metabolism that compensates for the reduced vascular supply.

In trying to elucidate the complex mechanisms responsible for resistance to anti-angiogenic therapy, our study also highlights the important contribution from using vascular imaging strategies that correctly inform on the extent and distribution of functional tumor vasculature. Furthermore, longitudinal monitoring of tumor fBV with susceptibility contrast MRI could facilitate expedient switching of VEGF receptor tyrosine kinase inhibitors as part of sequential therapeutic strategies designed to overcome acquired resistance, and which appear to be beneficial in the treatment of patients with mRCC (46, 47).

In conclusion, we have shown that quantitation of fBV using susceptibility contrast MRI provides a sensitive imaging biomarker for both predicting and assessing the response of 786-0 RCC xenografts to treatment with sunitinib. Clinical MRI investigations incorporating USPIO preparations are increasingly being performed, and determination of fBV may thus positively impact on mRCC patient stratification with anti-angiogenic therapy. In addition, we provide strong evidence that the phenotype of 786-0 xenografts exhibiting acquired resistance to sunitinib is not associated with functional re-vascularization *in vivo*.

Acknowledgements

We thank Allan Thornhill and his staff for animal care and maintenance.

References

1. Powles T, Chowdhury S, Jones R, Mantle M, Nathan P, Bex A, *et al.* Sunitinib and other targeted therapies for renal cell carcinoma. *Br J Cancer* **2011**;104:741-5.
2. Motzer RJ, Hutson TE, Tomczak P, Michaelson MD, Bukowski RM, Oudard S, *et al.* Overall survival and updated results for sunitinib compared with interferon- α in patients with metastatic renal cell carcinoma. *J Clin Oncol* **2009**;27:3584-90.
3. Motzer RJ, Hutson TE, Tomczak P, Michaelson MD, Bukowski RM, Rixe O, *et al.* Sunitinib versus interferon- α in metastatic renal-cell carcinoma. *New Engl J Med* **2007**;356:115-24.
4. Rini BI, Atkins MB. Resistance to targeted therapy in renal-cell carcinoma. *Lancet Oncol* **2009**;10:992-1000.
5. Bergers G, Hanahan D. Modes of resistance to anti-angiogenic therapy. *Nat Rev Cancer* **2008**;8:592-603.
6. Vasudev NS, Reynolds AR. Anti-angiogenic therapy for cancer: current progress, unresolved questions and future directions. *Angiogenesis* **2014**;17:471-94.
7. O'Connor JPB, Aboagye EO, Adams JE, Aerts HJWL, Barrington SF, Beer AJ, *et al.* Imaging biomarker roadmap for cancer studies. *Nat Rev Clin Oncol* **2017**;14:169-86.
8. O'Connor JPB, Rose CJ, Waterton JC, Carano RAD, Parker GJM, Jackson A. Imaging intratumor heterogeneity: role in therapy response, resistance, and clinical outcome. *Clin Cancer Res* **2015**;21:249-57.
9. O'Connor JPB, Jayson GC. Do imaging biomarkers relate to outcome in patients treated with VEGF inhibitors? *Clin Cancer Res* **2012**;18:6588-98.

10. Weissleder R, Elizondo G, Wittenberg J, Rabito C, Bengele H, Josephson L. Ultrasmall superparamagnetic iron oxide: characterization of a new class of contrast agents for MR imaging. *Radiology* **1990**;175:489-93.
11. Wu EX, Tang H, Jensen JH. Applications of ultrasmall superparamagnetic iron oxide contrast agents in the MR study of animal models. *NMR Biomed* **2004**;17:478-83.
12. Robinson SP, Howe FA, Griffiths JR, Ryan AJ, Waterton JC. Susceptibility contrast magnetic resonance imaging determination of fractional tumor blood volume: a noninvasive imaging biomarker of response to the vascular disrupting agent ZD6126. *Int J Radiat Oncol Biol Phys* **2007**;69:872-9.
13. Persigehl T, Wall A, Kellert J, Ring J, Remmele S, Heindel W, *et al.* Tumor blood volume determination by using susceptibility-corrected ΔR_2^* multiecho MR. *Radiology* **2010**;255:781-9.
14. Walker-Samuel S, Boulton JKR, McPhail LD, Box G, Eccles SA, Robinson SP. Non-invasive in vivo imaging of vessel calibre in orthotopic prostate tumour xenografts. *Int J Cancer* **2012**;130:1284-93.
15. Bridgeman VL, Wan E, Welti JC, Frentzas S, Foo S, Vermeulen PB, *et al.* Preclinical evidence that tremetinib enhances the response to anti-angiogenic tyrosine kinase inhibitors in renal cell carcinoma. *Mol Cancer Ther* **2015**;15:172-83.
16. Workman P, Aboagye EO, Balkwill F, Balmain A, Bruder G, Chaplin DJ, *et al.* Guidelines for the welfare and use of animals in cancer research. *Br J Cancer* **2010**;102:1555-77.
17. Kilkeny C, Browne WJ, Cuthill IC, Emerson M, Altman DG. Improving bioscience research reporting: The ARRIVE guidelines for reporting animal research. *PLoS Biol* **2010**;8:e1000412.

18. Welti JC, Powles T, Foo S, Gourlaouen M, Preece N, Foster J, *et al.* Contrasting effects of sunitinib within in vivo models of metastasis. *Angiogenesis* **2012**;15:623-41.
19. Walker-Samuel S, Orton M, McPhail LD, Boulton JKR, Box G, Eccles SA, *et al.* Bayesian estimation of changes in transverse relaxation rates. *Magn Reson Med* **2010**;64:914-21.
20. Tropres I, Lamalle L, Peoc'h M, Farion R, Usson Y, Decors M, *et al.* In vivo assessment of tumoral angiogenesis. *Magn Reson Med* **2004**;51:533-41.
21. Smith KA, Hill SA, Begg AC, Denekamp J. Validation of the fluorescent dye Hoechst 33342 as a vascular space marker in tumours. *Br J Cancer* **1988**;57:247-53.
22. Boulton JKR, Walker-Samuel S, Jamin Y, Leiper JM, Whitley GSJ, Robinson SP. Active site mutant dimethylarginine dimethylaminohydrolase 1 expression confers an intermediate tumour phenotype in C6 gliomas. *J Pathol* **2011**;225:344-52.
23. Altman DG. Practical statistics for medical research. London: Chapman and Hall/CRC; 1999.
24. Ferretti S, Allegrini PR, O'Reilly T, Schnell C, Stumm M, Wartmann M, *et al.* Patupilone induced vascular disruption in orthotopic rodent tumor models detected by magnetic resonance imaging and interstitial fluid pressure. *Clin Cancer Res* **2005**;11:7773-84.
25. Kostourou V, Robinson SP, Whitley GS, Griffiths JR. Effects of overexpression of dimethylarginine dimethylaminohydrolase on tumor angiogenesis assessed by susceptibility magnetic resonance imaging. *Cancer Res* **2003**;63:4960-6.
26. Persigehl T, Bieker R, Matuszewski L, Wall A, Kessler T, Kooijman H, *et al.* Antiangiogenic tumor treatment: early noninvasive monitoring with USPIO-enhanced MR imaging in mice. *Radiology* **2007**;244:449-56.

27. Nielsen T, Bentzen L, Pedersen M, Tramm T, Rijken PFJW, Bussink J, *et al.*
Combretastatin A-4 phosphate affects tumor vessel volume and size distribution as assessed using MRI-based vessel size imaging. *Clin Cancer Res* **2012**;18:6469-77.
28. Burrell JS, Walker-Samuel S, Baker LCJ, Boulton JKR, Jamin Y, Ryan AJ, *et al.*
Evaluation of novel combined carbogen USPIO (CUSPIO) imaging biomarkers in assessing the antiangiogenic effects of cediranib (AZD2171) in rat C6 gliomas. *Int J Cancer* **2012**;131:1854-62.
29. Bashir MR, Bhatti L, Marin D, Nelson RC. Emerging applications for ferumoxytol as a contrast agent in MRI. *J Magn Reson Imag* **2015**;41:884-98.
30. Ning P, Zucker EJ, Wong P, Vasanaawala SS. Hemodynamic safety and efficacy of ferumoxytol as an intravenous contrast agents in pediatric patients and young adults. *Magn Reson Imag* **2016**;34:152-8.
31. Nguyen K-L, Yoshida T, Han F, Ayad I, Reemtsen BL, Salusky IB, *et al.* MRI with ferumoxytol: A single center experience of safety across the age spectrum. *J Magn Reson Imag* **2017**;45:804-12.
32. Fredrickson J, Serkova NJ, Wyatt SK, Carano RAD, Pirzkall A, Rhee I, *et al.* Clinical translation of ferumoxytol-based vessel size imaging (VSI): Feasibility in a phase I oncology clinical trial population. *Magn Reson Med* **2017**;77:814-25.
33. Michaelis LC, Ratain MJ. Measuring response in a post-RECIST world: from black and white to shades of grey. *Nat Rev Cancer* **2006**;6:409-14.
34. Flaherty KT, A. Rosen M, F. Heitjan D, L. Gallagher M, Schwartz B, D. Schnall M, *et al.* Pilot study of DCE-MRI to predict progression-free survival with sorafenib therapy in renal cell carcinoma. *Cancer Biol Ther* **2008**;7:496-501.

35. Hahn OM, Yang C, Medved M, Karczmar G, Kistner E, Karrison T, *et al.* Dynamic contrast-enhanced magnetic resonance imaging pharmacodynamic biomarker study of sorafenib in metastatic renal carcinoma. *J Clin Oncol* **2008**;26:4572-8.
36. Fournier LS, Oudard S, Thiam R, Trinquart L, Banu E, Medioni J, *et al.* Metastatic renal carcinoma: evaluation of antiangiogenic therapy with dynamic contrast-enhanced CT. *Radiology* **2010**;256:511-8.
37. Han KS, Jung DC, Choi HJ, Jeong MS, Cho KS, Joung JY, *et al.* Pretreatment assessment of tumor enhancement on contrast-enhanced computed tomography as a potential predictor of treatment outcome in metastatic renal cell carcinoma patients receiving antiangiogenic therapy. *Cancer* **2010**;116:2332-42.
38. Cowey CL, Fielding JR, Kimryn Rathmell W. The loss of radiographic enhancement in primary renal cell carcinoma tumors following multitargeted receptor tyrosine kinase therapy is an additional indicator of response. *Urology* **2010**;75:1108-13.e1.
39. Smith AD, Lieber ML, Shah SN. Assessing tumor response and detecting recurrence in metastatic renal cell carcinoma on targeted therapy: importance of size and attenuation on contrast-enhanced CT. *Am J Roentgen* **2010**;194:157-65.
40. Schor-Bardach R, Alsop DC, Pedrosa I, Solazzo SA, Wang X, Marquis RP, *et al.* Does arterial spin-labelling MR imaging-measured tumor perfusion correlate with renal cell cancer response to antiangiogenic therapy in a mouse model? *Radiology* **2009**;251:731-42.
41. de Bazelaire C, Alsop DC, George D, Pedrosa I, Wang Y, Michaelson MD, *et al.* Magnetic resonance imaging-blood flow change after antiangiogenic therapy with PTK787/ZK222584 correlates with clinical outcome in metastatic renal cell carcinoma. *Clin Cancer Res* **2008**;14:5548-54.

42. Ebos JML, Kerbel RS. Antiangiogenic therapy: impact on invasion, disease progression, and metastasis. *Nat Rev Clin Oncol* **2011**;8:210-21.
43. McIntyre A, Harris AL. Metabolic and hypoxic adaptation to anti-angiogenic therapy: a target for induced essentiality. *EMBO Mol Med* **2015**;7:368-79.
44. O'Connor JPB, Boulton JKR, Jamin Y, Babur M, Finegan KG, Williams KJ, *et al.* Oxygen-enhanced MRI accurately identifies, quantifies, and maps tumor hypoxia in preclinical cancer models. *Cancer Res* **2016**;76:787-95.
45. Jiménez-Valerio G, Martínez-Lozano M, Bassani N, Vidal A, Ochoa-de-Olza M, Suárez C, *et al.* Resistance to antiangiogenic therapies by metabolic symbiosis in renal cell carcinoma PDX models and patients. *Cell Rep* **2016**;15:1134-43.
46. Choueiri TK, Escudier B, Powles T, Mainwaring PN, Rini BI, Donskov F, *et al.* Cabozantinib versus everolimus in advanced renal-cell carcinoma. *N Engl J Med* **2015**;373:1814-23.
47. Escudier B, Michaelson MD, Motzer RJ, Hutson TE, Clark JI, Lim HY, *et al.* Axitinib versus sorafenib in advanced renal cell carcinoma: subanalyses by prior therapy from a randomised phase III trial. *Br J Cancer* **2014**;110:2821-8.

Table and Legend

	786-0		786-0-R
	Pre-treatment	Post-treatment	Post-treatment
Volume (mm ³)	153 ± 17	148 ± 24	494 ± 44
fBV (%)	8.2 ± 2	2.4 ± 0.5**	2.2 ± 0.5

Table 1 – Summary of the quantitative volumetric and fractional blood volume (fBV) data acquired from 786-0 xenografts (n=9) prior to and 2 weeks after daily treatment with sunitinib, and from 786-0-R xenografts exhibiting acquired resistance to sunitinib (n=6). Data are mean ± 1 s.e.m., **p<0.01, paired t-test.

Figure Legends

Figure 1 – The anti-angiogenic activity of sunitinib in 786-0 RCC xenografts can be assessed *in vivo* using susceptibility contrast MRI. Parametric fractional blood volume (fBV) maps calculated from a 786-0 xenograft (a) prior to and (b) following 2 weeks of daily treatment with 40mg/kg sunitinib p.o. (c) Cumulative frequency curves of fBV obtained from the same 786-0 xenograft. The mean pre- and post-treatment fBV values for this tumor were 9.6 and 2.3%. (d) Line series of fBV determined for each 786-0 xenograft imaged prior to and post-treatment.

Figure 2 – Histological confirmation of the anti-angiogenic effects of sunitinib on vascular density and perfused vasculature of 786-0 RCC xenografts. (a) Microscopic images (x100) acquired from endomucin stained sections from control and sunitinib-treated 786-0 RCC xenografts, used to quantify MVD. A significantly lower MVD was determined in the sunitinib treated cohort (n=9) compared to control (n=5) (data are mean \pm 1 s.e.m., **p<0.01, unpaired t-test). (b) Composite fluorescence images of Hoechst 33342 uptake acquired from whole sections of control and sunitinib-treated 786-0 RCC xenografts, used to quantify the extent of functional (perfused) tumor vasculature. The area of Hoechst 33342 uptake was significantly lower in the sunitinib treated cohort compared to control (data are mean \pm 1 s.e.m., n=5 per treatment group, *p<0.05, unpaired t-test).

Figure 3 – Tumor fractional blood volume (fBV), quantified using susceptibility contrast MRI, is a predictive biomarker of subsequent response to sunitinib in 786-0 RCC xenografts. (a) Scatter graph of the average of the final and mean pre-treatment fBV plotted against the change in fBV in 786-0 xenografts measured 2 weeks after daily treatment with 40mg/kg sunitinib. Linear regression analysis and associated 95% confidence intervals are shown. A highly significant and strong negative correlation was obtained ($R^2 = 0.92$, $p < 0.0001$). (b) Scatter graph showing no relationship between

sunitinib-induced Δ fBV with change in tumor volume ($R^2 = 0.37$, $p=0.08$).

Figure 4 – Acquired resistance to sunitinib is not associated with rescue angiogenesis in 786-0 RCC xenografts. (a) Parametric fractional blood volume (fBV) maps obtained from two 786-0-R xenografts exhibiting acquired resistance to sunitinib acquired 62 (upper map) and 99 (lower map) days post initiation of daily treatment. The mean fBV for both tumors was 2.1%. The quantitative volumetric and fBV data acquired from the 786-0-R cohort are summarised and shown in comparison to that obtained from the 786-0 xenografts, and clearly shows that (b) despite the larger mean MRI-derived tumor volume compared to the post-treatment 786-0 tumors, (c) there was no difference in fBV. Data are the individual volumetric and fBV measurements from each tumor, and the cohort mean \pm 1 s.e.m.

Figure 1

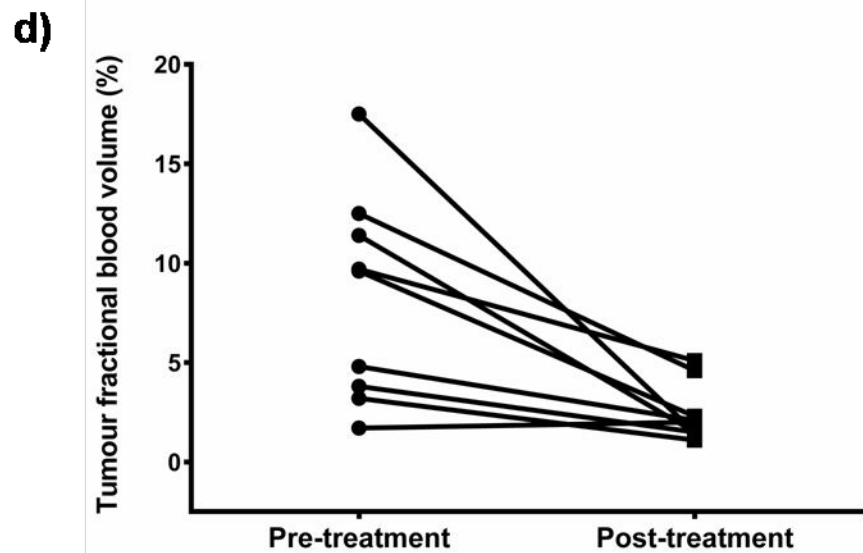
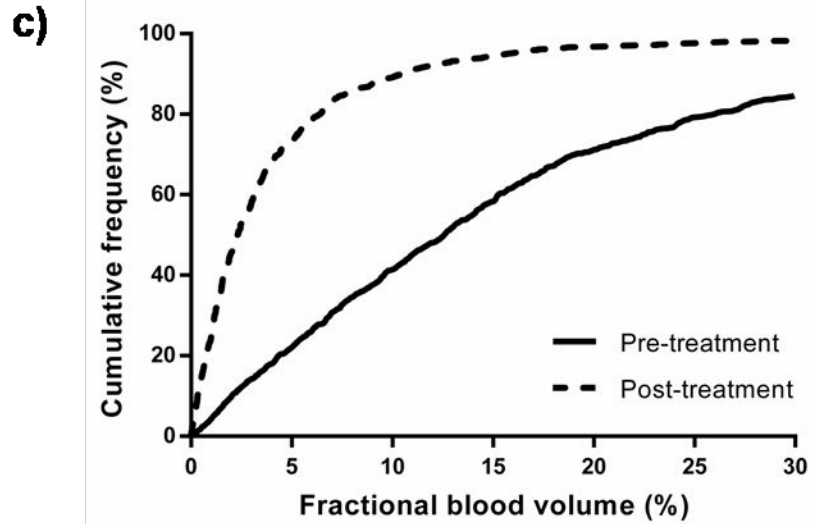
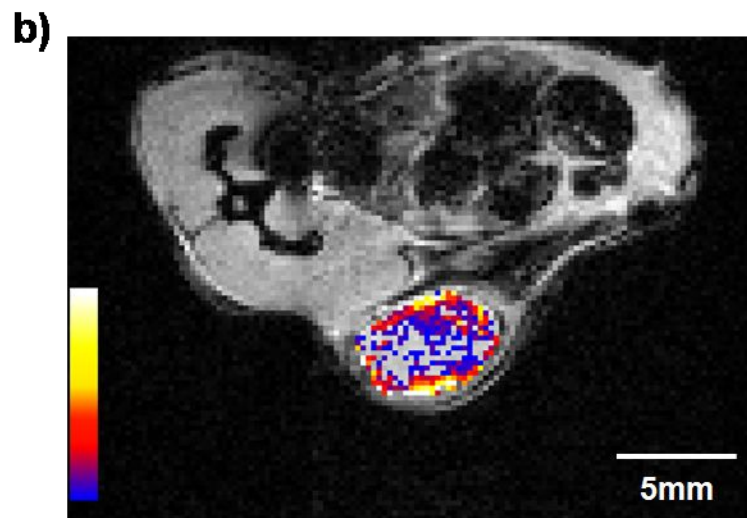
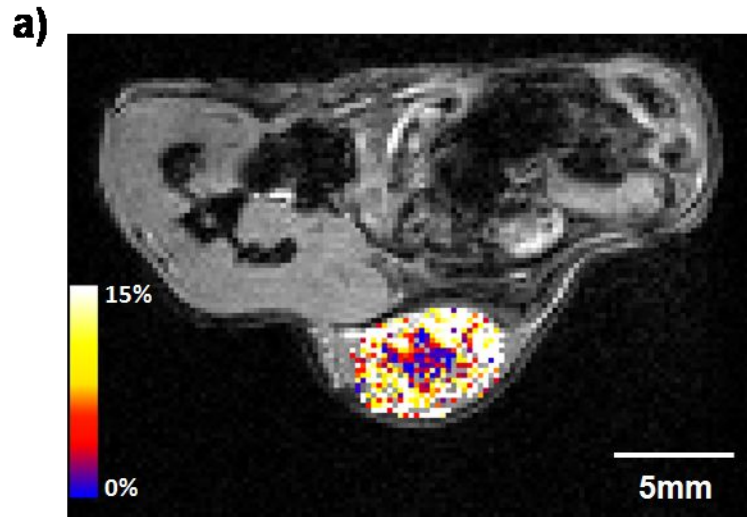
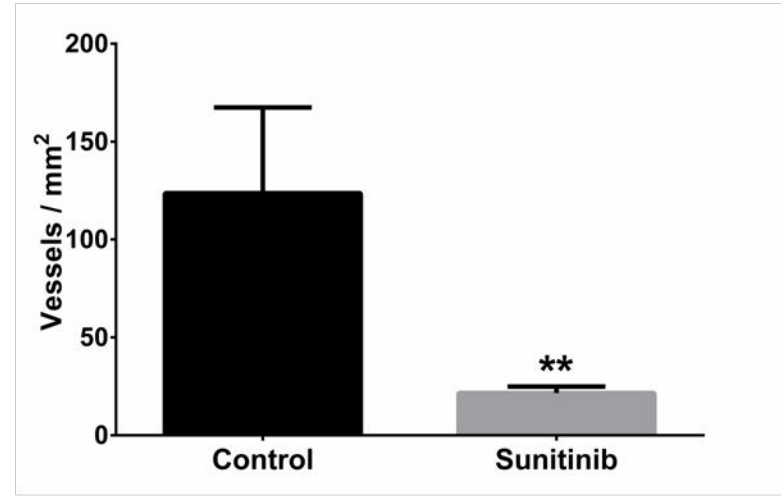
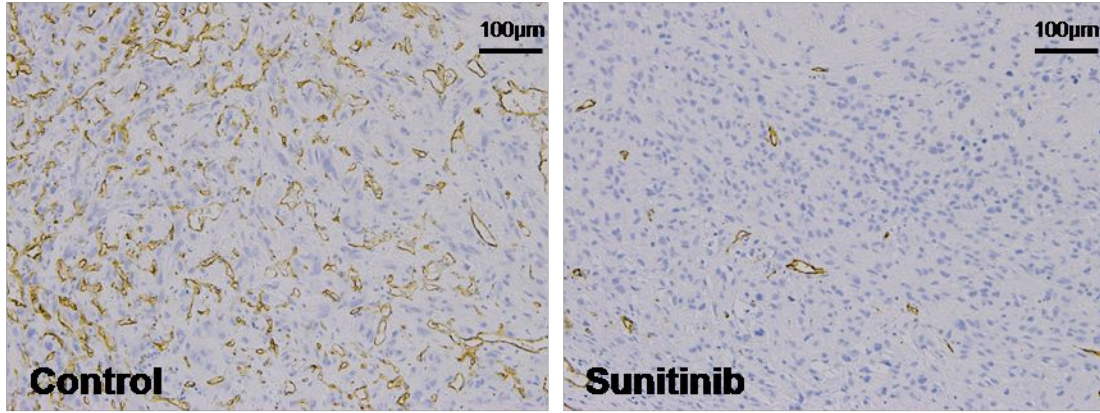


Figure 2

a)



b)

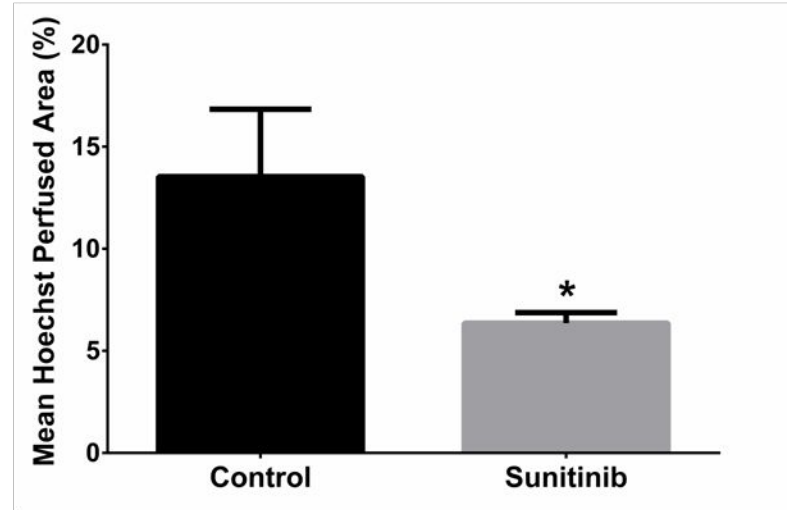
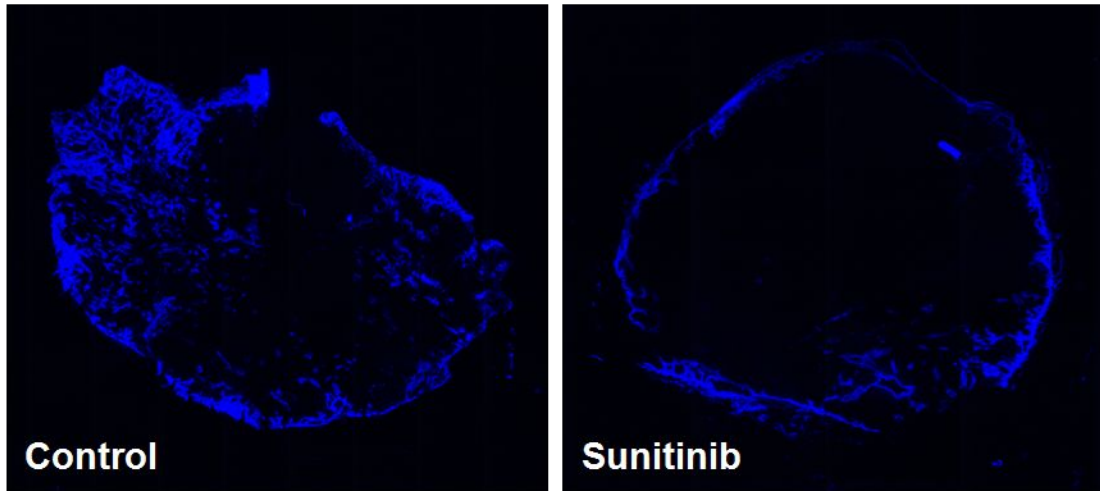


Figure 3

